RAA 2018 Vol. **18** No. **11**, 141(12pp) doi: 10.1088/1674–4527/18/11/141

http://www.raa-journal.org *http://iopscience.iop.org/raa*

***R**esearch in*
***A**stronomy and*
***A**strophysics*

Log-normal flux distribution of bright *Fermi* blazars

Zahir Shah[1], Nijil Mankuzhiyil[2], Atreyee Sinha[3,4], Ranjeev Misra[3], Sunder Sahayanathan[2] and Naseer Iqbal[1]

[1] Department Of Physics, University of Kashmir, Srinagar-190006, India; *shahzahir4@gmail.com*
[2] Astrophysical Sciences Division, Bhabha Atomic Research Centre, Mumbai-400085, India; *nijil@barc.gov.in*
[3] Inter-University Centre for Astronomy and Astrophysics, Pune-411007, India
[4] AstroParticule et Cosmoligie, CNRS/University Paris Diderot, 10 Rue Alice Domon et Leonie Duquet, Paris 75013, France

Received 2018 April 9; accepted 2018 June 6

Abstract We present the results of the γ-ray flux distribution study on the brightest blazars which were observed by *Fermi*-LAT. We selected 50 of the brightest blazars based on the maximum number of detections reported in the Third LAT AGN Catalog. We performed standard unbinned maximum likelihood analysis on the LAT data during the period between August 2008 and December 2016, in order to obtain the average monthly flux. After quality cuts, blazars for which at least 90% of the total flux had survived were selected for further study, and this included 19 FSRQs and 19 BL Lacs. The Anderson-Darling and χ^2 tests suggest that the integrated monthly flux follows a log-normal distribution for all sources, except for three FSRQs for which neither a normal nor a log-normal distribution was preferred. A double log-normal flux distribution tendency was observed in these sources, though this has to be confirmed with improved statistics. We also found that the standard deviation of the log-normal flux distribution increases with the mean spectral index of the blazar, and can be fitted with a line of slope 0.24 ± 0.04. We repeat our study on three additional brightest unclassified blazars to identify their flux distribution properties. Based on the features of their log-normal flux distribution, we infer these unclassified blazars may be closely associated with FSRQs. We also highlight that considering the log-normal behavior of the flux distribution of blazars, averaging their long term flux on a linear scale can largely underestimate the nominal flux and this discrepancy can propagate down to the estimation of source parameters through spectral modeling.

Key words: active galaxy: blazar — FSRQ — BL Lac — gamma-rays

1 INTRODUCTION

Blazars are a subclass of active galactic nuclei (AGNs) with their relativistic jets pointing towards the line of sight of the observer (Blandford & Königl 1979). Even though the mechanism behind the formation of relativistic jets is not fully understood yet, it is most likely related to focusing properties of the fully ionized, rotating accretion disk (Blandford & Znajek 1977). Blazars include BL Lacertae (BL Lac) objects and flat-spectrum radio quasars (FSRQs), with the significant difference between these two classes being their optical emission/absorption lines, which are strong for FSRQs, but weak or absent for BL Lacs (Urry & Padovani 1995).

The spectral energy distribution (SED) of blazars consists of two broad emission components, where the low energy component peaks at the optical to X-ray band, while the high energy component peaks at the MeV to TeV band. BL Lac objects are further subdivided based on the peak frequency ($\nu_{\rm s}$) of their low energy component, namely high energy peaked BL Lac (HBL; $\nu_{\rm s} > 10^{15.3}$ Hz), intermediate energy peaked BL Lac (IBL; $10^{14} < \nu_{\rm s} \leq 10^{15.3}$ Hz) and low energy

peaked BL Lac (LBL; $\nu_{\rm s} \leq 10^{14}$ Hz) (Fan et al. 2016). In case of FSRQs, $\nu_{\rm s}$ usually falls at relatively lower frequencies ($\lesssim 10^{14}$ Hz). The low energy component of a blazar SED is commonly attributed to synchrotron emission due to the interaction of relativistic electrons in the jet magnetic field; whereas the high energy component is explained as an inverse Compton (IC) scattering process. If the target low energy photon for the IC process is the synchrotron photon itself, then the IC mechanism is called synchrotron self Compton (SSC; Marscher & Gear 1985; Band & Grindlay 1985). On the other hand, if the photon origin is external to the jet, e.g. broad line region (BLR), obscuring torus, Cosmic Microwave Background (CMB), etc., then the process is called the external Compton (EC) mechanism (Dermer et al. 1992; Sikora et al. 1994; Shah et al. 2017). Alternate to this leptonic interpretation of the high energy emission, hadronic models involving nuclear cascades were also put forth and are successful in explaining many observed features of blazars (Mannheim & Biermann 1992; Böttcher 2007).

One of the distinct properties of blazars is their rapid flux and spectral variability across the entire electromagnetic spectrum on timescales ranging from minutes to years. Though the cause of variability is still not well understood, plausible clues can be obtained by studying the long term flux distribution of blazars. Such studies have been performed in detail at X-ray energies for Seyfert galaxies and X-ray binaries, where the emission at these energies is dominated by the accretion disk or its corona. The X-ray flux of Seyfert 1 IRAS 13224–3809, using *Advanced Satellite for Cosmology and Astrophysics* (*ASCA*) observations in different epochs, exhibits a log-normal distribution (Gaskell 2004). In another study, Uttley et al. (2005) found that the X-ray flux of Seyfert 1 NGC 4051 also shows a log-normal distribution, which is comparable to the X-ray flux of the black-hole X-ray binary Cyg X-1. A linear relationship between the optical flux and the corresponding variation was noticed in Seyfert 1 NGC 4151 (Lyutyj & Oknyanskij 1987), which in turn is an indication of log-normality of the flux distribution. A similar relationship was also noticed in the X-ray band in both Seyfert 1 Mrk 766 (Vaughan et al. 2003b) and Seyfert 2 MCG 6-30-15 (Vaughan et al. 2003a). The log-normality of flux distribution in a blazar was first detected in BL Lacertae, from *Rossi X-ray Timing Explorer* (*RXTE*) observations (Giebels & Degrange 2009). This result is particularly interesting since for blazars, X-ray emission originates from jets rather than the accretion disk or its environment. Hence, this result may hint at the plausible disk-jet connection in blazars, which is still not clearly understood. The log-normality was later observed in many blazars at different energies. For instance, such behavior was inferred in Mrk 421 and Mrk 501 at a Very High Energy (VHE $>$100 GeV) band, though the data were noncontinuous (Tluczykont et al. 2010). Similarly, the 4-year flux distribution of blazars, given in the Third LAT AGN Catalog (3LAC; Ackermann et al. 2015), showed a log-normal behavior. While quantifying the flux variability in Mrk 421, Sinha et al. (2016) also noticed a log-normal flux distribution (more than normal) trend, throughout the frequencies from radio to VHE. On the contrary, in a detailed multi-wavelength study of FSRQ PKS 1510–089, Kushwaha et al. (2016) found that the flux distribution follows two distinctive log-normal profiles in both optical and γ-rays, while the X-ray flux distribution follows a single log-normal distribution. Interestingly, the γ-ray flux distribution of the same source, obtained from nearly continuous data during August 2008-October 2015, was fitted well by a log-normal distribution, and similar were the cases of HBL Mrk 421 and FSRQs B2 1520+31. On the other hand, the γ-ray flux distribution of FR I radio galaxy NGC 1275 was not able to be represented by a log-normal or normal function, even though the rms increased linearly with flux (Kushwaha et al. 2017).

In this work, we aim to study the flux distribution properties of the brightest *Fermi* blazars using the data collected during more than 8 years. We also investigate the associated spectral properties of these brightest blazars. Further, we examine the above properties in order to associate the blazar candidates of uncertain type (BCUs) with known blazar classes. We select bright blazars from the 3LAC and analyze their data (described in Sect. 2). In order to overcome the effect of short-term flux variations, which are most likely associated with a change in emission region geometry, we consider the flux in monthly bins for our study. After analyzing features of the flux distribution and verifying the related log-normality (Sect. 3), we study the association of flux distribution with spectral properties (Sect. 4). The results and possible implications are discussed in Section 5.

2 *FERMI*-LAT ANALYSIS

The Large Area Telescope (LAT) on board the *Fermi* satellite is a pair conversion detector (Atwood et al.

2009) with an effective area of $\sim 8000\,\mathrm{cm^2\,GeV^{-1}}$ for on-axis photons, and field of view ~ 2.4 sr, in the energy range from 20 MeV to more than 300 GeV, which scans the entire sky every 3 hours. We made a primary selection of 25 FSRQs and 25 BL Lacs from NASA's four year Fermi 3LAC interactive table[1]. The selection was based on criteria such that the chosen FSRQs and BL Lacs should have monthly averaged photon flux $> 6.5 \times 10^{-9}\,\mathrm{photons\,cm^{-2}\,s^{-1}}$ and $> 5.5\times10^{-9}\,\mathrm{photons\,cm^{-2}\,s^{-1}}$ respectively, and the number of upper limits (i.e, non-detections) should be less than or equal to 4. We then downloaded the first 8.4 years of data (from August 2008 to December 2016) for the selected sources. The data were analyzed in the energy range from 100 MeV to 500 GeV, in a region of interest of 10° centered on the nominal source positions. The analysis was carried out using the maximum likelihood method (*gtlike*) and standard *Fermi* SCIENCE TOOLS (version v9r12) with the instrument response function 'P8R2_SOURCE_V6', Galactic diffuse model 'gll_iem_v06.fit' and isotropic background model 'iso_p8R2_SOURCE_V6_v06.txt'. Events which were contaminated by a bright Earth limb were excluded using a zenith angle cut of 90°. Further, the time bins with $\mathrm{TS} < 9$ were excluded, which correspond to a detection significance of $\sqrt{\mathrm{TS}} \approx 3\sigma$. We estimated monthly photon flux, energy flux and spectral index for all the sources using maximum likelihood analysis.

3 FLUX DISTRIBUTION

The monthly average γ-ray flux obtained in the analysis of ~ 100 months of data was distributed into a histogram of fluxes for each source. An adaptive binning was used for each source to ensure the bin width is larger than the average error of the flux within a bin. Apart from the flux that corresponds to a test statistic (TS) value $\mathrm{TS} \leq 9$, we also excluded the flux with larger uncertainty, such that $F/\delta F < 2$. In order to avoid bias due to a possible lack of lower luminosity flux states, we restrict our focus to the blazars for which the total excluded flux points (after the cuts mentioned above) are less than 10%. After this cut, 38 (out of 50) blazars survived, which include 19 BL Lacs and 19 FSRQs.

[1] *https://fermi.gsfc.nasa.gov/ssc/data/access/lat/4yr_ catalog/3FGL-table/*

We fit all 38 flux histograms in log-scale, with functions

$$L(x) = \frac{1}{\sqrt{2\pi}\sigma} \exp^{\frac{-(x-\mu)^2}{2\sigma^2}}$$

[would give log-normal distribution in log-scale] (1)

and

$$G(x) = \frac{1}{\sqrt{2\pi}\sigma} \exp^{\frac{(10^x-\mu)^2}{2\sigma^2}} 10^x \log_e(10)\ ,$$

[would give normal distribution in log-scale] (2)

where σ and μ are the standard deviation and mean of the distribution, respectively.

The flux histograms of the blazars are plotted on log-scale in Figure 1. The normal and log-normal fits are shown as red and blue lines respectively. Figure 2 (left panel) displays the comparison between reduced χ^2 obtained from normal and log-normal distributions. The fit parameters together with the computed skewness for both distributions are shown in Table 1. The flux distributions are found to be significantly skewed, whereas the skewness of the log of the flux distribution is consistent with zero, thus suggesting a log-normal trend (Fig. 2, right panel). Apart from calculating the reduced χ^2, we have also performed an Anderson-Darling (AD) test, in order to verify the normality/log-normality of the fits. The reduced χ^2 of the fit, together with the AD test statistics and rejection/null hypothesis probability (p-value) are also shown in Table 1.

We note that the reduced χ^2 for the normal flux distribution of some of the blazars falls in a reasonable range. However, the p-value estimated from the AD test rejects the normal distribution ($p < 0.05$) for all sources, except for the FSRQ J0957.6+5523 (with a highly reduced χ^2 in this case). On the other hand, the AD test p-value and the reduced χ^2 of the flux distribution of J0957.6+5523 do not reject the log-normal distribution of flux either. It is interesting to note that the χ^2 and AD tests do not reject the log-normality of the flux distribution of most of the blazars. Nevertheless, both tests reject the log-normality of the flux distribution of FSRQs J2329.3–4955, J1504.4+1029 and J1625.7–2527. Even though the AD tests marginally (e.g., J1427.9–4206) and completely (J1512.8–0906) reject the log-normal fits of a few blazar flux distributions, the corresponding χ^2 values are reasonable enough not to reject the log-normality.

The standard deviation obtained from the log-normal fits, which is a measure of flux variability, is com-

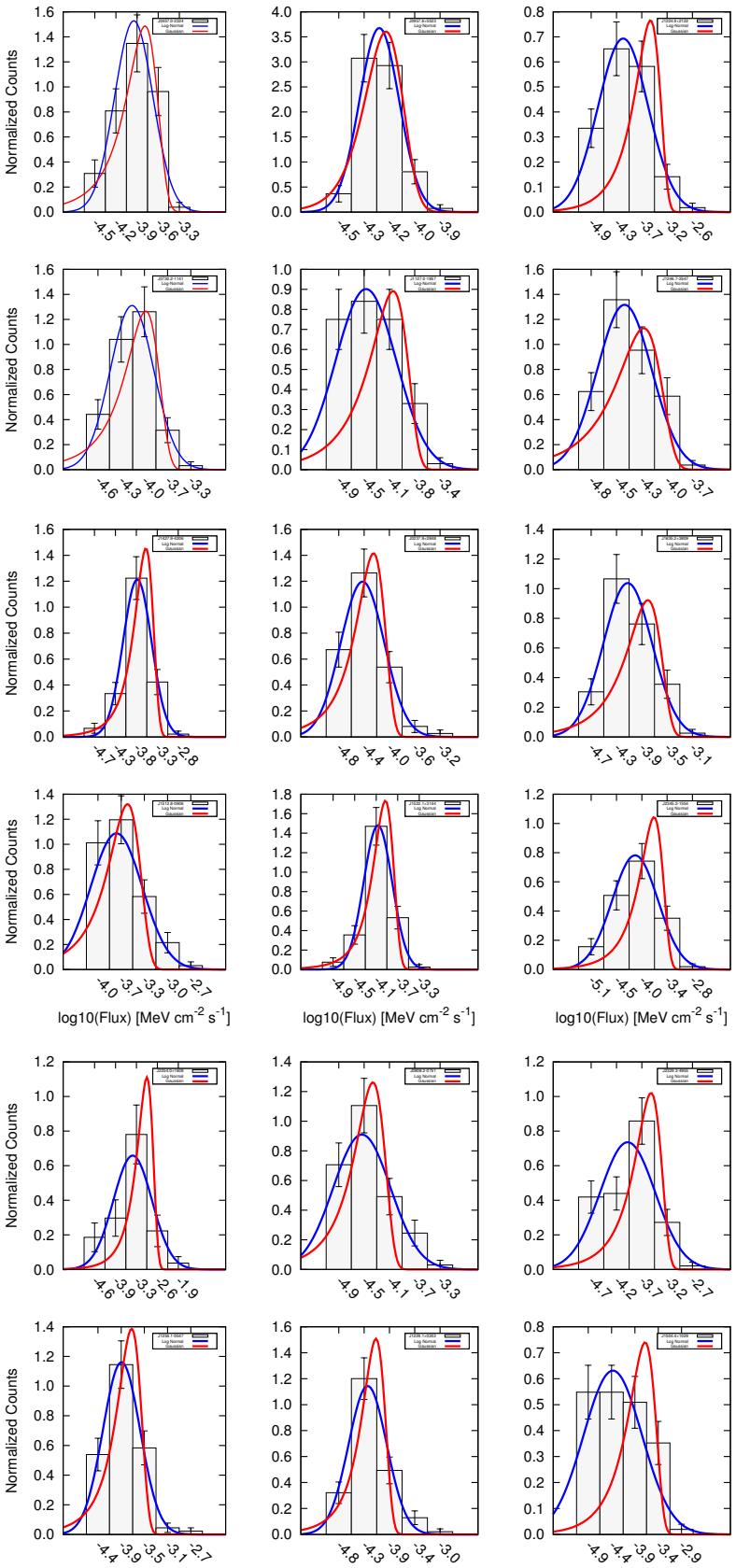

Fig. 1 Flux distribution of bright blazars in the γ-ray band. The *blue* and *red lines* correspond to log-normal and normal fits respectively.

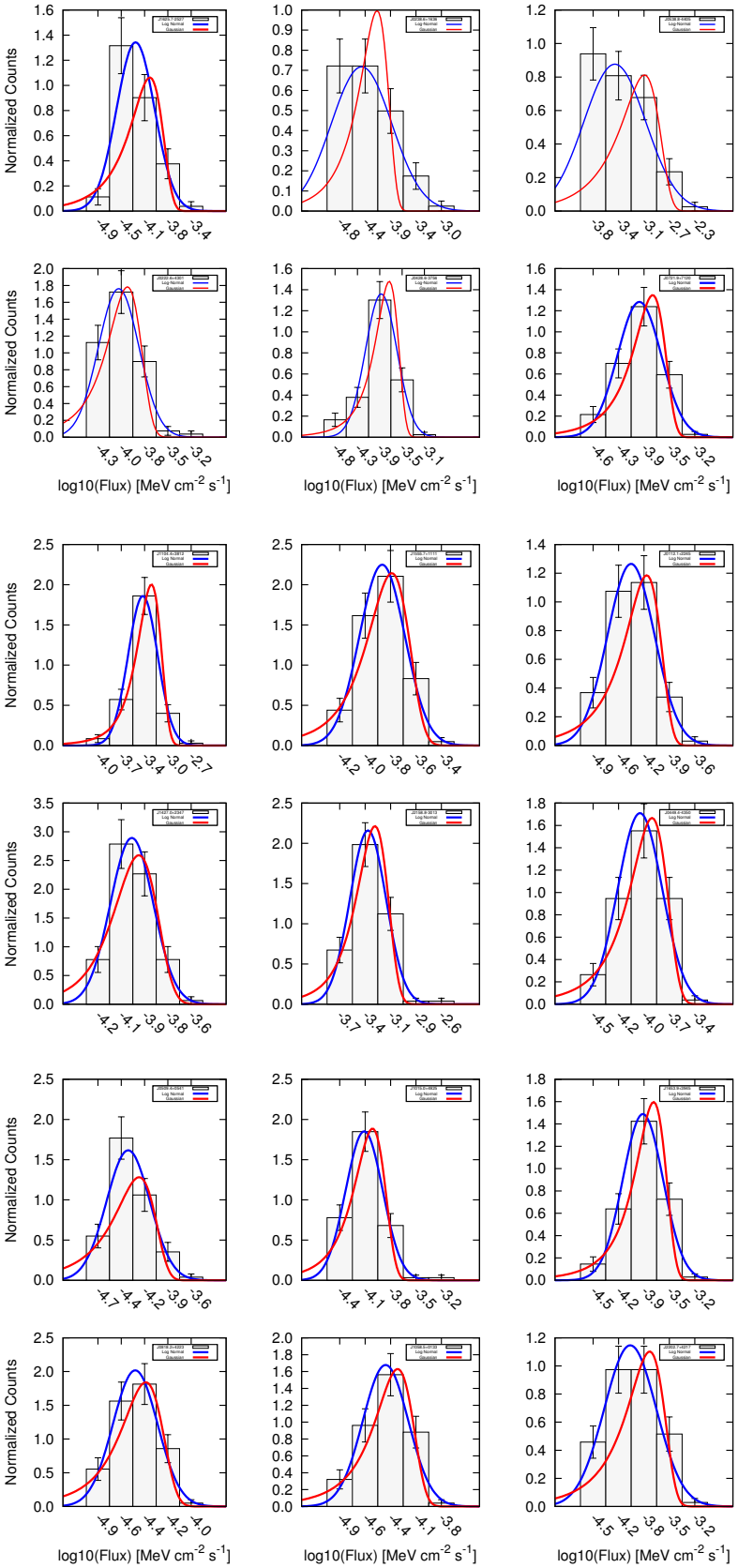

Fig. 1 — *Continued.*

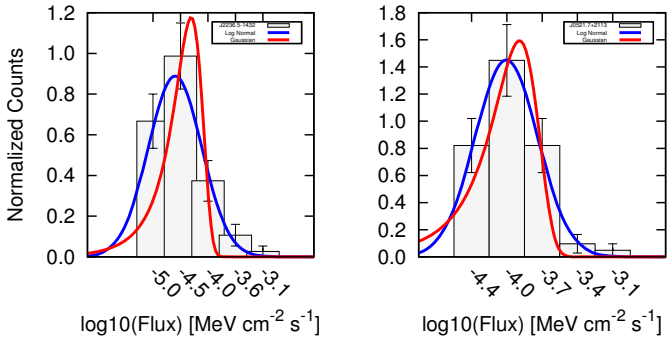

Fig. 1 — *Continated.*

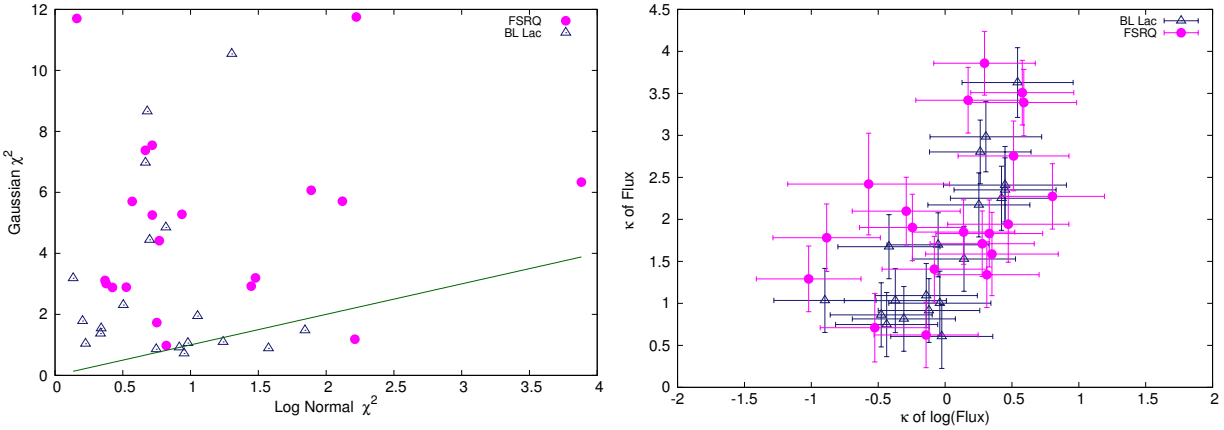

Fig. 2 *Left*: the reduced χ^2 obtained from the blazar flux distribution by fitting a log-normal distribution (x axis) and normal distribution (y axis). The *pink circles* represent FSRQs, while *blue triangles* stand for BL Lacs. The *green line* corresponds to the condition $y = x$. *Right*: computed skewnesss from the log-normal distribution (x axis) and normal distribution (y axis).

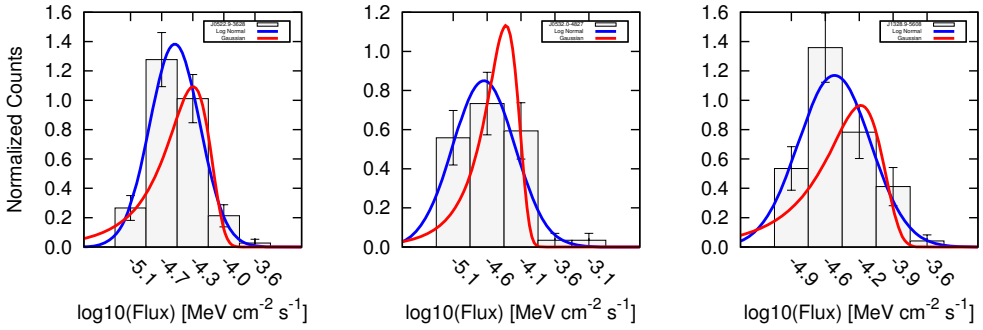

Fig. 3 Flux distribution of bright blazars in γ-ray band. The line styles are the same as in Fig. 1.

paratively high for FSRQs. In the case of BL Lacs, HBLs show a lower variability, while the variability of LBLs is similar to that of FSRQs. The variability of IBLs roughly falls in between those of HBLs and LBLs. The mean values of the standard deviation obtained from the log-normal fit of the considered FSRQs, HBLs, IBLs and LBLs are 0.41±0.11, 0.21±0.04, 0.27±0.03 and 0.37±0.10 respectively. We have also noticed that the standard deviation of the flux distribution of J0957.6+5523 is significantly smaller compared to other FSRQs, so it could be treated as a *steady FSRQ*.

3.1 The Case of Uncertain Type Blazars

More than 500 sources were classified as BCUs in 3LAC. Even though these sources are associated with extragalactic counterparts and show some blazar character-

Table 1 The fitting parameters of log-normal (columns 2 and 3) and normal (columns 7 and 8) flux distribution of blazars. The computed skewness (columns 4 and 9), reduced χ^2 (columns 5 and 10) and AD statistics (columns 6 and 11) for both distributions are also shown.

FSRQ										
Blazar	Log-normal					Normal				
Name	Width	Centroid	Skewness (κ)	χ^2/dof	AD (prob)	Width*	Centroid*	Skewness*	χ^2/dof	AD (prob)
(1)	(2)	(3)	(4)	(5)	(6)	(7)	(8)	(9)	(10)	(11)
J0457.0–2324	0.26±0.03	–3.96±0.04	–0.52±0.40	2.21	0.64 (0.09)	8.33±1.40	11.1±1.60	0.71±0.40	1.12	1.50 (6.7e–04)
J0730.2–1141	0.30±0.02	–4.17±0.02	–0.08±0.39	0.42	0.37 (0.41)	6.39±1.17	6.71±2.01	1.40±0.39	2.88	3.32 (2.3e–08)
J0957.6+5523	0.12±0.01	–4.24±0.01	–0.14±0.39	0.53	0.22 (0.84)	1.54±0.21	5.85±0.28	0.62±0.39	2.89	0.69 (0.07122)
J1127.0–1857	0.45±0.04	–4.49±0.06	0.33±0.39	0.67	0.72 (0.06)	6.48±2.04	3.17±3.18	1.83±0.39	7.38	6.40 (7.7e–16)
J1224.9+2122	0.57±0.02	–4.17±0.03	0.17±0.39	0.16	0.33 (0.51)	23.8±8.34	8.26±17.6	3.41±0.39	11.7	10.97 (<2.2e–16)
J1246.7–2547	0.30±0.03	–4.45±0.04	0.31±0.39	0.93	0.72 (0.06)	3.79±1.08	3.25±1.50	1.34±0.39	5.21	5.44 (1.6e–13)
J1427.9–4206	0.33±0.02	–3.75±0.03	–0.88±0.40	0.75	1.02 (0.01)	15.2±3.28	19.6±5.39	1.78±0.40	1.73	4.61 (1.6e–11)
J1512.8–0906	0.37±0.04	–3.73±0.05	–0.80±0.38	0.71	2.44 (3.2e–06)	15.7±4.52	17.6±6.85	2.27±0.38	5.26	10.36 (<2.2e–16)
J0237.9+2848	0.33±0.02	–4.43±0.02	0.59±0.39	0.36	0.71 (0.06)	3.04±0.77	3.78±1.22	3.39±0.39	3.11	5.44 (1.6e–13)
J2254.0+1608	0.60±0.10	–3.37±0.12	–0.57±0.60	1.44	0.83 (0.03)	78.7±47.1	66.4±96.9	2.42±0.60	2.92	4.65 (9.7e–12)
J1522.1+3144	0.27±0.02	–4.07±0.02	–1.02±0.39	0.84	0.62 (0.10)	5.58±0.65	9.13±0.96	1.29±0.39	0.90	2.11 (2.1e–05)
J1635.2+3809	0.38±0.03	–4.14±0.03	0.27±0.39	0.72	0.76 (0.05)	11.1±3.45	6.49±5.65	1.71±0.39	7.54	6.78 (<2.2e–16)
J2329.3–4955	0.54±0.10	–3.97±0.14	–0.24±0.39	3.88	1.09 (0.01)	21.7±6.67	15.6±12.9	1.90±0.39	6.33	4.16 (2.0e–10)
J2345.2–1554	0.51±0.03	–4.10±0.04	–0.29±0.40	0.56	0.22 (0.84)	14.5±5.63	10.7±9.85	2.09±0.40	5.70	6.66 (<2.2e–16)
J0808.2–0751	0.45±0.05	–4.53±0.06	0.51±0.41	0.77	0.65 (0.09)	2.72±0.78	2.71±1.25	2.75±0.41	4.42	8.46 (<2.2e–16)
J1229.1+0202	0.34±0.04	–4.28±0.04	0.57±0.38	1.48	0.70 (0.06)	3.89±1.25	5.29±1.93	3.50±0.38	3.12	12.89 (<2.2e–16)
J1256.1–0547	0.34±0.02	–3.94±0.02	0.29±0.37	0.38	0.27 (0.68)	9.92±2.83	11.9±4.16	3.86±0.37	3.01	8.63 (<2.2e–16)
J1504.4+1029	0.63±0.10	–4.38±0.15	0.14±0.38	2.22	0.98 (0.01)	17.9±7.48	5.29±11.4	1.84±0.38	11.7	8.54 (<2.2e–16)
J1625.7–2527	0.30±0.04	–4.28±0.05	0.47±0.45	2.12	1.11 (0.01)	5.96±1.88	4.64±2.98	1.94±0.45	5.71	6.87 (<2.2e–16)
BL Lac										
J0222.6+4301	0.23±0.02	–4.04±0.02	0.45±0.38	0.50	0.44 (0.28)	5.23±1.07	8.88±1.42	2.35±0.38	2.30	3.55 (6.1e–09)
J0238.6+1636	0.56±0.06	–4.42±0.08	0.30±0.42	0.67	0.85 (0.03)	5.19±2.04	3.57±2.97	2.98±0.42	6.97	7.70 (<2.2e–16)
J0428.6–3756	0.33±0.03	–3.95±0.04	–0.90±0.38	1.84	11.45 (0.01)	9.75±2.14	11.5±2.83	1.03±0.38	1.47	2.15 (1.7e–05)
J0538.8–4405	0.45±0.06	–3.48±0.08	0.42±0.38	1.30	1.02 (0.01)	73.1±27.3	30.5±40.2	2.25±0.38	10.5	8.04 (<2.2e–16)
J0721.9+7120	0.31±0.02	–3.96±0.03	–0.37±0.38	1.05	0.66 (0.08)	9.66±1.75	11.1±2.56	1.03±0.38	1.94	2.25 (9.7e–06)
J1104.4+3812	0.21±0.02	–3.39±0.02	–0.42±0.38	0.91	0.48 (0.22)	23.0±1.89	45.1±3.15	1.67±0.38	0.92	2.67 (8.9e–07)
J1427.0+2347	0.14±0.01	–4.00±0.01	–0.02±0.38	0.20	0.34 (0.50)	3.74±0.56	9.92±0.68	0.61±0.38	1.78	1.13 (0.01)
J1555.7+1111	0.17±0.01	–3.84±0.01	–0.04±0.38	0.22	0.5124 (0.19)	6.88±0.78	14.6±0.97	1.00±0.38	1.04	2.12 (2.1e–05)
J2158.8–3013	0.18±0.01	–3.38±0.02	0.25±0.38	0.75	0.1918 (0.89)	19.1±2.52	42.2±2.75	2.17±0.38	0.86	2.68 (8.4e–07)
J0112.1+2245	0.31±0.01	–4.42±0.01	–0.05±0.38	0.13	0.14 (0.97)	4.06±0.76	3.50±1.31	1.70±0.38	3.19	4.21 (9.2e–11)
J0449.4–4350	0.23±0.02	–4.02±0.03	–0.44±0.38	1.57	0.51 (0.20)	6.35±0.80	9.55±0.93	0.75±0.38	0.89	1.11 (0.01)
J0509.4+0541	0.25±0.02	–4.36±0.02	0.14±0.39	0.69	0.19 (0.89)	3.63±0.95	3.65±1.27	1.53±0.39	4.44	3.02 (1.2e–07)
J0818.2+4223	0.20±0.01	–4.52±0.02	–0.12±0.38	0.95	0.26 (0.72)	1.61±0.16	3.02±0.18	0.91±0.38	0.72	2.05 (3.0e–05)
J1015.0+4925	0.22±0.01	–4.09±0.01	0.26±0.38	0.34	0.31 (0.56)	4.45±0.66	8.11±0.97	2.80±0.38	1.36	3.94 (7.1e–10)
J1058.5+0133	0.25±0.03	–4.43±0.04	–0.31±0.39	1.24	0.45 (0.27)	2.70±0.43	3.83±0.41	0.82±0.39	1.09	2.67 (8.6e–07)
J1653.9+3945	0.28±0.02	–2.88±0.03	–0.48±0.38	0.98	0.63 (0.10)	9.33±1.22	13.6±1.58	0.86±0.38	1.06	1.30 (2.1e–3)
J2202.7+4217	0.35±0.03	–4.02±0.04	–0.14±0.38	0.81	0.74 (0.05)	11.6±3.02	9.69±4.56	1.09±0.38	4.85	2.82 (3.8e–07)
J2236.5–1432	0.41±0.03	–4.51±0.04	0.54±0.42	0.68	0.63 (0.10)	7.91±2.48	2.23±4.92	3.63±0.42	8.65	12.24 (<2.2e–16)
J0521.7+2113	0.28±0.02	–4.05±0.02	0.45±0.46	0.34	0.38 (0.39)	6.06±1.26	8.30±1.66	2.41±0.46	1.54	3.69 (2.6e–09)

Note: * unit of 10^{-5} MeV cm^{-2} s^{-1}.

istics, they lack reliable classification based on spectral information. In order to investigate the flux distribution properties of such sources, we analyzed long term data (in the same time period as that of the other bright blazars) for three of the brightest BCUs (namely, J0522.9–3628, J0532.0–4827 and J1328.9–5608). These sources are comparatively less bright than the known classified blazars that we considered. After analyzing the *Fermi*-LAT data of these three bright BCUs with the standard *Fermi* SCIENCE TOOL and using the quality cuts, i.e. the flux after the cuts of $F/\delta F < 2$ and TS ≤ 9, it was not possible to match with the acceptance criterion of 90%. Therefore, we modified our acceptance criterion from 90% to 60% of the total flux. Since the flux states

with TS<9 belong to low flux states (quiescent states) or less variable states, this difference in the acceptance criterion will not significantly bias our final results. The flux distribution of all three sources suggests log-normal distributions. The reduced χ^2 values of the log-normal flux distribution for the sources J0522.9–3628, J0532.0–4827 and J1328.9–5608 are found to be 0.29, 1.18 and 0.73 respectively (instead of 5.67, 3.09 and 5.79 respectively in the case of a normal distribution). The AD test statistic p-values of the logarithmic flux distribution for the sources (in the same order as above) are 0.78, 0.80 and 0.17 respectively (instead of 6.72×10^{-15}, 2.86×10^{-16} and 2.37×10^{-11} respectively for the normal distribution), which also support log-normal distributions of flux over normal distributions. The obtained standard deviations from the log-normal fit of J0522.9–3628 and J1328.9–5608 are 0.29 and 0.34 respectively, while it is high (0.47, which is similar to FSRQs and LBLs) for the source J0532.0–4827.

4 ASSOCIATION OF FLUX DISTRIBUTION WITH SPECTRAL INDEX

In order to investigate the association of flux variability with spectral indices, we estimated the monthly spectra of the blazars. All the considered blazars were well described by either simple power law or log parabola models. In order to compare the spectral indices of the spectra described by both models, it would be meaningful to calculate the spectral indices at a specific energy, which was chosen to be 1 GeV (denoted by $\alpha_{1\,\mathrm{GeV}}$). The spectral index at energy E is defined by

$$\alpha_{\mathrm{E}} = \alpha + 2\beta \log(E/E_{\mathrm{p}}) \ , \qquad (3)$$

where α is spectral index at pivot energy E_{p} and β is the measure of spectral curvature. We have found that the average spectral index for all FSRQs is 2.28±0.03. However, the FSRQ J2254.0+1608 (a.k.a. 3C 454.3, which is the brightest blazar in the γ-ray band) shows a harder spectral index of 1.72±0.06. It has to be also noted that the spectral index of the *steady FSRQ* J0957.6+5523 is also smaller, 1.91±0.05. The mean spectral indices of all other FSRQs fall in the range 2.08–2.75. However, the mean spectral indices of BL Lacs fall in the range 1.61–2.49, with a mean value of 2.01±0.11.

The mean spectral indices of BCUs J0522.9–3628, J0532.0–4827 and J1328.9–5608 are 2.70, 2.64 and 2.74 respectively. These values fall in the range of spectral indices for other bright FSRQs, LBLs or IBLs, but are comparatively higher than the spectral indices of HBLs.

The flux variability has been plotted against the spectral index in Figure 4. The HBLs (red squares) fall in the lower-left corner of the diagram, while FSRQs (pink circles) show a wider distribution. The IBLs (green triangles) and LBLs (gray asterisks) fall in a similar range of spectral index, though the variability distribution is wider in the case of the former. The boxes represent two-standard deviation uncertainty in $\alpha_{1\,\mathrm{GeV}}$ and σ from their respective mean values. The bright BCUs that were analyzed fall in the band of FSRQs. We also notice a slight correlation between the spectral index and standard deviation of the flux. The $\alpha_{1\,\mathrm{GeV}}$ and σ of all blazars can be roughly fitted by a straight line with slope 0.24±0.04, which is indicated by a blue dotted line in Figure 4. The brightest BCUs show similar features as in the case of other blazars with respect to spectral index and flux distribution. All three BCUs (indicated as purple diamonds in Fig. 4) fall beyond the 2-standard deviation uncertainty region (dotted box) of BL Lac sources. However, they are placed within the 2-standard deviation uncertainty region of FSRQs.

Additionally, we have also compared the monthly spectral indices of each source with their corresponding luminosity. It is interesting to note that every source shows the *harder when brighter* phenomenon. The monthly spectral indices and corresponding luminosity can be fitted well by a straight line. The average indices are found to be $-0.09 + 0.01$ for FSRQs, while they are –0.11±0.01, –0.13±0.01 and –0.13±0.01 for HBLs, IBLs and LBLs respectively, suggesting the *harder when brighter* phenomenon among the different bright blazar classes is not significantly different.

5 DISCUSSION

After a detailed study of the γ-ray flux of 38 of the brightest blazars, we found that the flux distributions predominantly suggest a log-normal distribution rather than a normal distribution. We verified the log-normality (over normality) using both reduced χ^2 and AD test. The log-normality was rejected only in the case of three (in a sample of 38) blazars. However, the normal distribution was rejected for all blazars (except J0957.6+5523, though the reduced χ^2 was high). The flux distribution of the three brightest BCUs follows a log-normal distribution. From the obtained spectral index and the flux standard deviation parameters, they fall beyond the 2-standard devia-

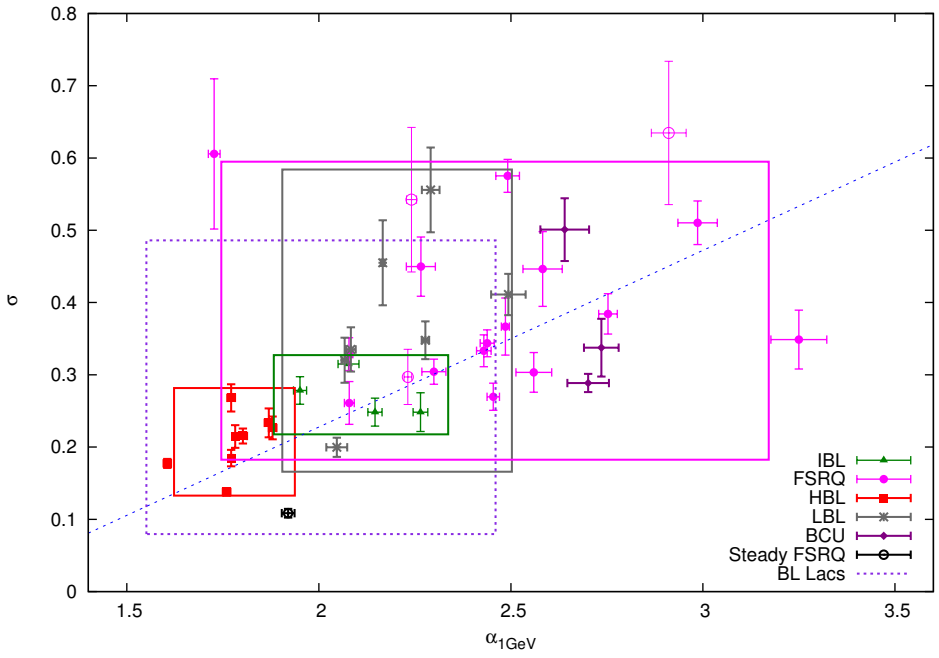

Fig. 4 The standard deviation (σ) of the blazar flux distribution vs. their corresponding average spectral index at 1 GeV ($\alpha_{1\,\mathrm{GeV}}$). Each blazar class has been marked with different symbols. HBL: *red filled squares*, IBL: *green triangles*, LBL: *gray asterisks*, FSRQ: *pink circles* and BCU: *purple diamonds*. The FSRQs which reject the log-normal flux distribution have been marked as *pink open circles*. The *steady FSRQ* has been shown separately as a *black filled circle*. The *rectangular boxes* correspond to two-standard-deviation uncertainty from the mean of σ and $\alpha_{1\,\mathrm{GeV}}$ for each blazar class. The color of a given box is chosen to be the same as that of the symbols for each blazar class. The *blue-violet dotted box* corresponds to two-standard-deviation uncertainty from the mean of σ and $\alpha_{1\,\mathrm{GeV}}$ for all BL Lac sources.

tion uncertainty limits of HBLs, IBLs and LBLs. Though it cannot be asserted, we are tempted to associate these sources with FSRQs.

The log-normal distribution of the observed flux indicates the perturbation associated with the emission process to be of multiplicative nature rather than additive (Lyubarskii 1997; Arévalo & Uttley 2006). Flux variation in blazars can be attributed to the complex interplay between the intrinsic and source parameters. A simple scenario is to associate the flux variation with the fluctuation in the emitting electron number density or the magnetic field. However, the linear dependence of these quantities with the differential flux suggests this will cause a normal flux distribution, contrary to the observations. Alternatively, the particle acceleration and diffusion processes can modify the shape of the emitting electron distribution (Kirk et al. 1998) and hence can account for various flux distributions, including a log-normal one. The flux variation can also be associated with the change in emission region geometry. Even though the change in volume associated with this can only produce a normal flux distribution, inclusion of light travel time effects can significantly modify the same (Chiaberge & Ghisellini 1999). However, the timescales associated with these processes are too short and hence will not reflect the log-normal distribution obtained in our study, where we used monthly averaged fluxes.

A log-normal flux distribution can directly hint at the linkage of blazar jet with the accretion phenomenon since the latter has been demonstrated to produce such a distribution through the study of Galactic X-ray binaries (XRBs) (Uttley & McHardy 2001). Fluctuations in the disk at different radii are known to be produced independently by viscosity fluctuation on local viscous timescales, which modulates the mass accretion rate at larger distances from a black hole. The accretion rate variations then propagate to small radii through accretion flow and variations at different radii result in multiplicative emission. This model was put forward by Lyubarskii (1997) for an explanation of the observed X-ray variability timescales in XRBs. Also, for non-beamed accreting objects the variability timescales are found to be proportional to $M/\dot{m}$, where M is the mass of the black hole and $\dot{m}$ is the accretion rate (Körding et al.

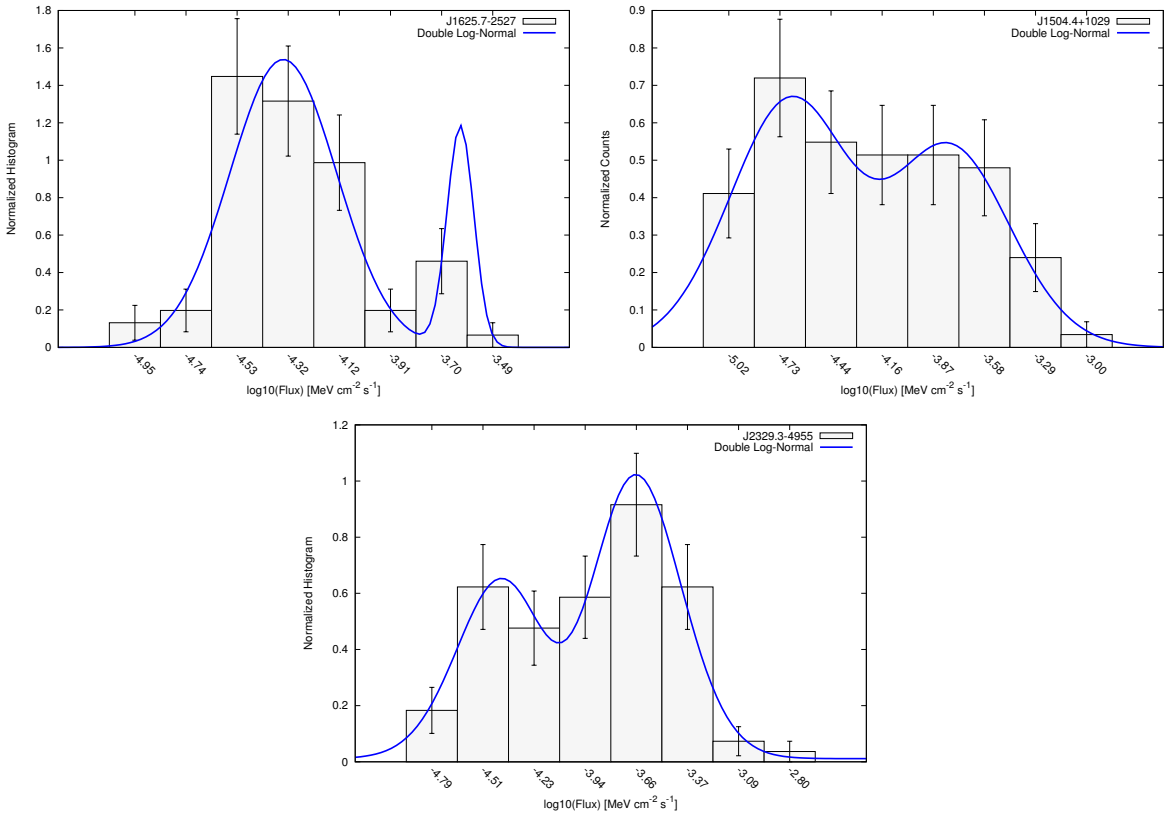

Fig. 5 Double log-normal fit to the flux distribution of the blazars J1625.7–2527, J1504.4+1029 and J2329.3–4955, which reject a log-normal distribution. Since the statistics are not significant enough, these fits should be taken only as indicative.

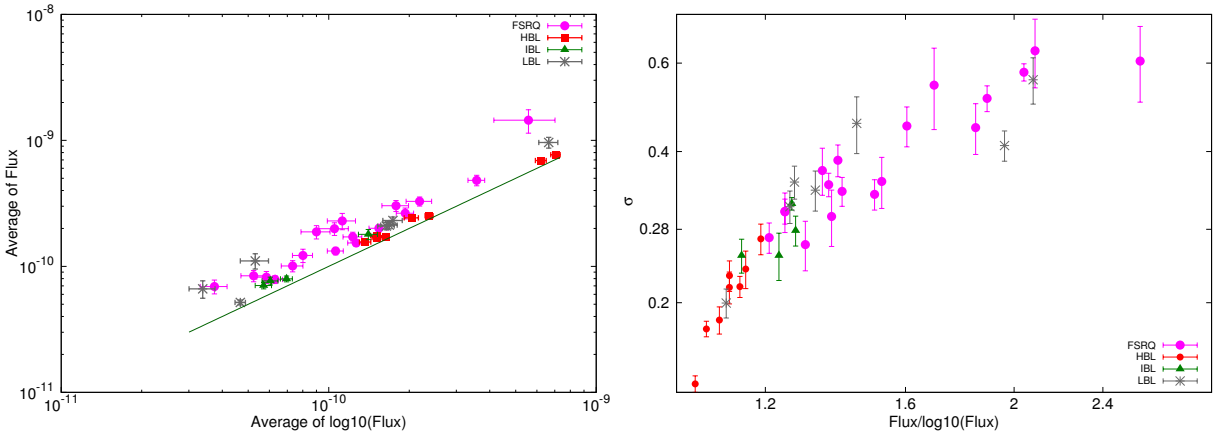

Fig. 6 Left plot shows the average of flux vs. average of logarithm of flux for bright blazars. The line represents the condition of equality of quantities. On the right, standard deviation of the log-normal flux distribution is plotted against the ratio between flux and logarithm of flux. Color for each symbol indicates the blazar class, *pink*: FSRQ, *red*: HBL, *green*: IBL and *gray*: LBL.

2007). McHardy (2008) concluded that the same relation surprisingly holds even for beamed jet emission from blazars, e.g. 3C 273, which should have otherwise shorter observed variability timescale due to relativistic time dilation than the timescale predicted using the black hole mass and accretion rate. Consequently, this leads to the inference that the source of variations in blazars lies outside the jet, i.e. in the accretion disk which then modulates the jet emission. A detailed study of month scale averaged flux distribution of blazars can hence be a key to understand the disk-jet connection.

Contrary to the interpretations above, a log-normal flux distribution can also arise from additive processes under specific conditions. For example, if the blazar jet is assumed to be a large collection of mini-jets, then the logarithm of composite flux will show a normal distribution (Biteau & Giebels 2012).

We note that the AD statistics do not reject the normality of the flux distribution for J0957.6+5523. Moreover, the standard deviation obtained from the flux distribution of this source exhibits a significant difference from that of other blazars. 3LAC labeled this source as an FSRQ, based on the presence of broad optical emission lines, large redshift and high γ-ray luminosity of the order of $\approx 10^{47}\,\mathrm{erg\,s^{-1}}$. However, the integrated spectrum and morphological properties obtained from the VLBA observations question the FSRQ classification of the source and suggest it to be one of the weakest Compact Symmetric Objects (Rossetti et al. 2005). Moreover, the brightness temperature of this source was found to be significantly lower (2×10^8 K at 5 GHz, Taylor et al. 2007) than that of other γ-ray blazars (McConville et al. 2011). These studies, together with our results, suggest that more multi-wavelength studies are required before associating this source with an FSRQ.

We have also investigated the possibility of a double log-normal distribution of fluxes for the sources that reject a log-normal distribution both in χ^2 and AD tests (J1625.7–2527, J1504.4+1029 and J2329.3–4955). The two distinct log-normal profiles may indicate different flux states corresponding to low and high states of the source (Kushwaha et al. 2016). It is interesting to note that the flux distribution of all three sources exhibits hints of a double log-normal distribution (Fig. 5). However, the statistics of this distribution are not significant enough, hence these results should be taken only as an indicator.

Another implication of our study is on the averaging of long term flux. We recommend using the average of flux in log scale rather than estimating the average flux in a linear scale, especially for highly variable sources. We show the difference of averaged flux in both linear and log-scale in Figure 6. For example, in the case of FSRQs, the average value of Flux/Log_{10} (Flux) falls around $\sim$1.7, while the maximum value (in the case of 3C 454.3) goes up to 2.8. These values imply that averaging flux over a linear scale will significantly overestimate the same, which would in turn give rise to inaccurate SED non-thermal emission model parameters.

6 CONCLUSIONS

We studied the flux distribution properties of 38 of the brightest γ-ray blazars in detail using *Fermi*-LAT data spanning more than 8 years. The flux distribution suggests a log-normal distribution for 35 blazars, indicating a multiplicative perturbation associated with the emission process. Similar features were obtained also in the case of BCUs. On the other hand, the flux distributions of three FSRQs – J2329.3–4955, J1504.4+1029 and J1625.7–2527 – reject both log-normal and normal distributions. This could be due to two or more independent flux states associated with the source, however, more statistics are required to study these effects in detail. It would also be interesting to perform an elaborate study with better statistics for more blazars in γ-rays, and compare the properties with those of their X-ray counterparts.

Acknowledgements ZS, SS and NI are thankful to the Indian Space Research Organization program (ISRO-RESPOND) for the financial support (Grant No. ISRO/RES/2/396).

References

Ackermann, M., Ajello, M., Atwood, W. B., et al. 2015, ApJ, 810, 14
Arévalo, P., & Uttley, P. 2006, MNRAS, 367, 801
Atwood, W. B., Abdo, A. A., Ackermann, M., et al. 2009, ApJ, 697, 1071
Band, D. L., & Grindlay, J. E. 1985, ApJ, 298, 128
Biteau, J., & Giebels, B. 2012, A&A, 548, A123
Blandford, R. D., & Königl, A. 1979, ApJ, 232, 34
Blandford, R. D., & Znajek, R. L. 1977, MNRAS, 179, 433
Böttcher, M. 2007, Ap&SS, 309, 95
Chiaberge, M., & Ghisellini, G. 1999, MNRAS, 306, 551
Dermer, C. D., Schlickeiser, R., & Mastichiadis, A. 1992, A&A, 256, L27
Fan, J. H., Yang, J. H., Liu, Y., et al. 2016, ApJS, 226, 20
Gaskell, C. M. 2004, ApJ, 612, L21
Giebels, B., & Degrange, B. 2009, A&A, 503, 797
Kirk, J. G., Rieger, F. M., & Mastichiadis, A. 1998, A&A, 333, 452
Körding, E. G., Migliari, S., Fender, R., et al. 2007, MNRAS, 380, 301
Kushwaha, P., Chandra, S., Misra, R., et al. 2016, ApJ, 822, L13
Kushwaha, P., Sinha, A., Misra, R., Singh, K. P., & de Gouveia Dal Pino, E. M. 2017, ApJ, 849, 138
Lyubarskii, Y. E. 1997, MNRAS, 292, 679
Lyutyj, V. M., & Oknyanskij, V. L. 1987, AZh, 64, 465
Mannheim, K., & Biermann, P. L. 1992, A&A, 253, L21

Marscher, A. P., & Gear, W. K. 1985, ApJ, 298, 114
McConville, W., Ostorero, L., Moderski, R., et al. 2011, ApJ, 738, 148
McHardy, I. 2008, in Blazar Variability across the Electromagnetic Spectrum, 14
Rossetti, A., Mantovani, F., Dallacasa, D., Fanti, C., & Fanti, R. 2005, A&A, 434, 449
Shah, Z., Sahayanathan, S., Mankuzhiyil, N., et al. 2017, MNRAS, 470, 3283
Sikora, M., Begelman, M. C., & Rees, M. J. 1994, ApJ, 421, 153
Sinha, A., Shukla, A., Saha, L., et al. 2016, A&A, 591, A83
Taylor, G. B., Healey, S. E., Helmboldt, J. F., et al. 2007, ApJ, 671, 1355
Tluczykont, M., Bernardini, E., Satalecka, K., et al. 2010, A&A, 524, A48
Urry, C. M., & Padovani, P. 1995, PASP, 107, 803
Uttley, P., & McHardy, I. M. 2001, MNRAS, 323, L26
Uttley, P., McHardy, I. M., & Vaughan, S. 2005, MNRAS, 359, 345
Vaughan, S., Edelson, R., Warwick, R. S., & Uttley, P. 2003a, MNRAS, 345, 1271
Vaughan, S., Fabian, A. C., & Nandra, K. 2003b, MNRAS, 339, 1237